Journal of Catalysis **184,** 406–420 (1999)
Article ID jcat.1999.2466, available online at http://www.idealibrary.com on IDEAL®

Catalysis on Pd/WO_3 and Pd/WO_2: Effect of the Modifications of the Surface States Due to Redox Treatments on the Skeletal Rearrangement of Hydrocarbons

Part I. Physical and Chemical Characterizations of Catalysts by BET, TPR, XRD, XAS, and XPS

C. Bigey, L. Hilaire, and G. Maire[1]

Laboratoire d'Etudes de la Réactivité Catalytique, des Surfaces et Interfaces, UMR 7515 du CNRS, ECPM, Université Louis Pasteur, 4 rue Blaise Pascal, 67070 Strasbourg Cedex, France

Received October 20, 1998; revised January 19, 1999; accepted January 20, 1999

Bulk and surface properties of Pd/WO_3 and Pd/WO_2 catalysts were studied using temperature programmed reduction, X-ray diffraction, X-ray absorption, and X-ray photoelectron spectroscopies. Special attention was paid to the oxidation state of tungsten upon reduction under hydrogen at 350 and 600°C. The influence of oxidation treatments was also studied. Our results showed that reduction at 350°C led to the tranformation of bulk WO_3 into the stable $W_{20}O_{58}$ phase. At higher reduction temperature and also at 350°C, if the support WO_3 was calcined before impregnation, metallic tungsten was detected and we postulated that this transformation starts with the formation of the metastable W_3O phase via $W_{20}O_{58}$. All these transformations concern the surface as well as the bulk for Pd/WO_3 catalysts and the WO_3 contamination layer only for Pd/WO_2 catalyst. WO_2 seems more difficult to reduce than WO_3 even if the latter becomes less reducible after oxidation treatment. Autoreduction of the palladium salt was suggested on these catalysts, resulting both from the pretreatment of the supports and the nature of the Pd salt. Addition of a metal to bulk oxides facilitates their reducibility and allows one to obtain a stable surface state.

Key Words: **Pd/WO_3, Pd/WO_2 catalysts; hydrocarbons cracking; isomerization; surface states; mechanisms; TPR; XPS; XAS.**

1. INTRODUCTION

Catalysts containing tungsten oxides have been investigated in various reactions: olefins metathesis (1–3), propene oxidation (4), butene isomerization (5–8), hydrodesulfurization (9, 10), or NO*x* reduction (11). Recent studies showed that tungsten oxides seem to be potential catalysts for skeletal rearrangements of hydrocarbons (12–15). Some studies have shown a modification of the properties under H_2, due to the reducibility of the oxides. No stable state has yet been reported, to our knowledge. Hovewer, some correlations between the oxidation state of tungsten and the catalytic properties have been proven. Hydrocracking of *n*-heptane on WO_3 was investigated by Ogata *et al.* (12). Their results suggested that many reaction mechanisms occurred during the reduction under H_2 at various temperatures and were correlated with the presence of $WO_{3-\alpha}$, $WO_{3-\beta}$ ($\alpha < \beta < 1$), WO_2, and with W metal. The role of trace amounts of oxygen and water in the reaction mixture leading to isomerization in the conversion reaction of *n*-heptane on a WO_{3-x} phase was confirmed. Other authors (13–15) have shown that WO_3 was inactive towards hexanes isomerization and concluded that WO_3 had no dehydrogenation and consequently no isomerization properties. So an induction time under H_2 was necessary to obtain conversion of alkanes, which was correlated with the appearance of the WO_2 phase exhibiting a metallic character. Thus, we have turned our attention to palladium supported on bulk tungsten oxides. The presence of palladium was expected to improve the catalyst stability but also to activate the isomerization toward saturated hydrocarbons. Various studies were devoted to the interaction of transition metals (Pd, Pt) with tungsten oxides, leading to modifications of the activity (16–19) or the metal dispersion as compared to classical catalysts (17, 20–24). The metal was also reported to accelerate the reduction of the oxides and spillover processes were invoked (25–29).

The present paper is divided into two parts. First, we studied as a function of various treatments the reduction behaviour of tungsten oxides when palladium was added and the modifications of Pd induced by the oxide. Temperature programmed reduction (TPR), X-ray diffraction (XRD), X-ray absorption (XAS), and X-ray photoelectron spectroscopies (XPS) were used to characterize the catalysts (this paper). A second part will be devoted to the correlations of the catalytic properties for reforming hexanes and hexenes with the surface states evidenced in the present paper.

[1] To whom correspondence should be addressed.

0021-9517/99 $30.00

2. EXPERIMENTAL

2.1. Catalysts Preparation

The supported catalysts were prepared by "wet" impregnation of the tungsten oxides supports with an aqueous solution of tetrammine palladium II chloride in order to obtain 1 wt% Pd in the final sample. $Pd(NH_3)_4Cl_2,H_2O$ was provided by Johnson & Matthey. WO_3 and WO_2 supports were supplied by Strem Chemicals. The initial specific surface areas are, respectively, 1.5 and 0.15 m^2/g. Previous studies by XPS have reported that the surface of WO_2 was easily oxidized consecutively to an exposure to air and was contaminated by some WO_3 layers. With regard to this observation, the WO_2 support was submitted to a prereduction to favour as much as possible a clean WO_2 surface before the impregnation with the Pd salt. The same treatment was applied to prepare a Pd/WO_3 catalyst for comparison. The catalysts were identified as $Pd/(WO_3calc)$, $Pd/(WO_3red)$, and $Pd/(WO_2red)$.

$Pd/(WO_3calc)$. WO_3 bulk was submitted to a treatment in air flow at 400°C for 15 h. After cooling down to room temperature, the support was impregnated by the palladium salt. The excess of solvent was evaporated and the catalyst calcined under an air flow at 400°C for 4 h after drying. A heating rate of 10°C/min was used.

$Pd/(WO_3red)$. Prior to Pd deposition, WO_3 bulk was reduced in hydrogen at 350°C for 15 h with a heating rate of 10°C/min. After cooling down to room temperature, the catalyst was kept under an argon flow to prevent any reoxidation. The WO_3 support was then impregnated rapidly and the catalyst was only dried at 110°C overnight. This was used for catalytic tests without any calcination step.

$Pd/(WO_2red)$. The catalyst was prepared as $Pd/(WO_3red)$ using WO_2 as support.

The bulk oxides references WO_3 and WO_2 were used without any treatment. Table 1 summarizes the catalysts, metal and chlorine contents, and pretreatments.

2.2. Catalysts Characterization

BET. Specific surface areas were measured before and after various treatments in a Coulter SA 3100 BET apparatus. The weight of the catalyst varied between 200 and 500 mg, depending on the surface area of the sample. All catalysts were previously outgassed at 250°C for one hour. Nitrogen was adsorbed at −190°C.

TPR. Temperature programmed reduction analyses were performed in an XSORB (IFP-Gira) apparatus. Five percent hydrogen in argon, purified on molecular sieves, was used as a reducing agent, with a 25 cc/min flow. One hundred milligrams of sample were placed in a quartz reactor. The temperature was increased at the rate of 8°C/min up to 900°C where it remained steady for 2 h (TPR900). The sample was then cooled down to room temperature. In all cases pure oxygen was then introduced and the temperature was increased up to 400°C at a rate of 10°C/min. After cooling down to room temperature a new TPR experiment was performed. The samples were also calcined under the same conditions before any TPR experiment and three successive TPR were recorded for each sample, which can be summarized as:

"as prepared catalyst" submitted to TPR900 → TPRa

TPRa followed by an oxidation at 400°C plus TPR900 → TPRb

TPRb followed by an oxidation at 400°C plus TPR900 → TPRc.

H_2 consumption was measured by means of a catharometric detector.

XRD. X-ray diffraction spectra were recorded after various treatments on a Siemens D5000 apparatus using a Cu $K\alpha$ radiation over a 2θ range of 20° to 90°. Samples were treated *ex situ* under H_2 at 350°C for 15 h (LTR) or reduced at 600°C for 15 h (HTR). In some cases, we performed further oxidation under air at 400°C (O400) or under a $[O_2 + H_2O + N_2]$ mixture which was composed of 225 ppm O_2 and 80 ppm H_2O in N_2 (calibrated by mass spectrometry).

XAS. X-ray absorption spectroscopy experiments were performed at the synchrotron facility in Orsay (LURE) on the DCI EXAFS4 beam line. The W L_{III} edge (10207 eV) was recorded in transmission mode using a Si(111) or a Si(311) double monochromator and two ionization chambers as detectors. $Pd/(WO_3red)$ and $Pd/(WO_2red)$, together with reference samples diluted in γ-Alumina, were

TABLE 1

Weight Percentages of Metal and Chlorine and Methods of Pretreatments for the Supports before Impregnation

Catalysts	Pd (wt%)	Cl (wt%)	Pretreatment of the supports	Pretreatment of the catalysts
$Pd/(WO_3calc)$	0.87	560 ppm	calcined 400°C, 15 h	calcined 400°C, 4 h
$Pd/(WO_3red)$	0.93	0.65	reduced 350°C, 15 h	dried 110°C, overnight
$Pd/(WO_2red)$	0.93	0.48	reduced 350°C, 15 h	dried 110°C, overnight

analyzed at room temperature before and after *in situ* treatments under H_2, [$O_2 + H_2O + N_2$], and a mixture of H_2 and hydrocarbon (HC). The HC used was the 2,2-dimethylhexane ($PHC/PH_2 = 20/740$ torr). The energies were calibrated using a W polycrystalline foil. Qualitative analysis of only the W edge was performed. XANES spectra were normalized using the Michalowicz procedure by fitting a linear function to the pre-edge data, fitting a polynomial spline to the data of EXAFS region, extrapolating both functions to zero energy, taking the difference, and normalizing the data to unit step height (30).

XPS. X-ray photoelectron spectroscopy analyses were performed in a VG ESCA III spectrometer using the Al $K\alpha$ radiation. The samples, pressed into pellets, were attached to a nickel sample holder. Reductions under hydrogen and oxidations under air were performed at atmospheric pressure in a separate chamber directly connected to the spectrometer so that no air contamination took place between the treatments and the analyses. The evolution of the surface was followed as a function of time under hydrogen, usually in 4-h steps, until a stable surface was obtained; that is, no modification was observed after further reduction. The base pressure in both chambers was in the 10^{-10} range.

The binding energy reference was the C 1s peak at 284.8 eV. Calculations of the surface concentrations were performed by measuring the surface areas corrected from the photoionization cross sections (Scofield) and a square approximation was used to account for the differences in escape depths.

Reduction of WO_3 under hydrogen resulted in complicated spectra, due to the formation of various oxides which were identified and quantified by curve fitting analysis using a Doniach–Sunjic line shape (31). The binding energies of the various species and the parameters of the analysis were determined using reference spectra whenever possible: W, WO_2 (covered with WO_3), WO_3. The percentages of the various contributions were deduced from the surface areas with an accuracy which can be estimated to a few percent.

3. RESULTS AND INTERPRETATION

Unless otherwise specified, characterization studies (and catalytic experiments) were performed on samples "as prepared," that is, after drying overnight in an oven at 110°C for Pd/(WO_3red) and Pd/(WO_2red) and after calcination at 400°C for Pd/(WO_3calc), and on samples reduced under one atmosphere of hydrogen at two temperatures: 350 and 600°C (hereafter referred to as LTR and HTR, low and high temperature, respectively). In some cases a calcination under one atmosphere of air at 400°C took place after the low temperature reduction and was followed by a new low temperature reduction. Other experiments involved heating at 350°C in the mixture [$O_2 + H_2O + N_2$] previously described. Let us recall that Pd/(WO_3red) and Pd/(WO_3calc) refer to "as prepared" samples whose support was reduced under hydrogen at 350°C or calcined under air at 400°C, respectively.

TABLE 2

Specific Surface Areas of Catalysts after LTR and HTR Treatments

Catalysts	BET (m^2/g)		
	As prepared	LTR	HTR
Pd/(WO_3calc)[a]	7	8	6
Pd/(WO_3red)[a]	5	11	5
Pd/(WO_2red)[b]	1	1	4

[a] Specific surface area of WO_3 bulk support 1.5 m^2/g.
[b] Specific surface area of WO_2 bulk support 0.15 m^2/g.

3.1. BET

Table 2 gives the surface areas of the samples before and after 15 h of low and high temperature reduction. All surfaces were very small and a large difference is observed between Pd/WO_3 and Pd/WO_2 catalysts initially before any treatment. The lowest values were obtained with Pd/(WO_2red). Such a difference was also observed on bulk WO_3 and WO_2 oxides which is probably due to the difference in the structure of these bulk oxides.

Calcination and reduction treatments resulted in an increase in these surfaces by a factor of 5–7 whatever the oxide. Further reduction treatment of the catalysts did not lead to significant changes in surface areas.

3.2. TPR

Figure 1 gives the temperature progammed reduction results for the reference compound WO_3 and the two Pd/WO_3 samples (Pd/(WO_3calc) and Pd/(WO_3red)). Three successive hydrogen consumption profiles were recorded, as explained in the experimental section. It must be stressed that when the temperature reached 900°C, it was stabilized and the reduction was carried out for two more hours. This explains why the shape of the 900°C peaks was quite different.

The oxide WO_3 has a complicated profile exhibiting five peaks at 572, 635, 707, 871, and 900°C (Fig. 1) showing that the reduction of WO_3 proceeds in several steps. After oxidation three peaks only were detected at 707, 792, and 900°C. The total hydrogen consumption per mole of tungsten oxide gave a H_2/WO_3 ratio in the first step equal to 2.7 (Table 3) which corresponds to an almost complete reduction of WO_3 into metallic W, considering the reaction $WO_3 + 3H_2 \rightarrow W + 3H_2O$. This value decreased during the two steps to 2.0 and 1.5, respectively, which is probably due to an incomplete reoxidation of tungsten. We observed a slight shift of the peak at 871°C (TPRa) towards lower temperatures (792°C) after reoxidation. TPR patterns of

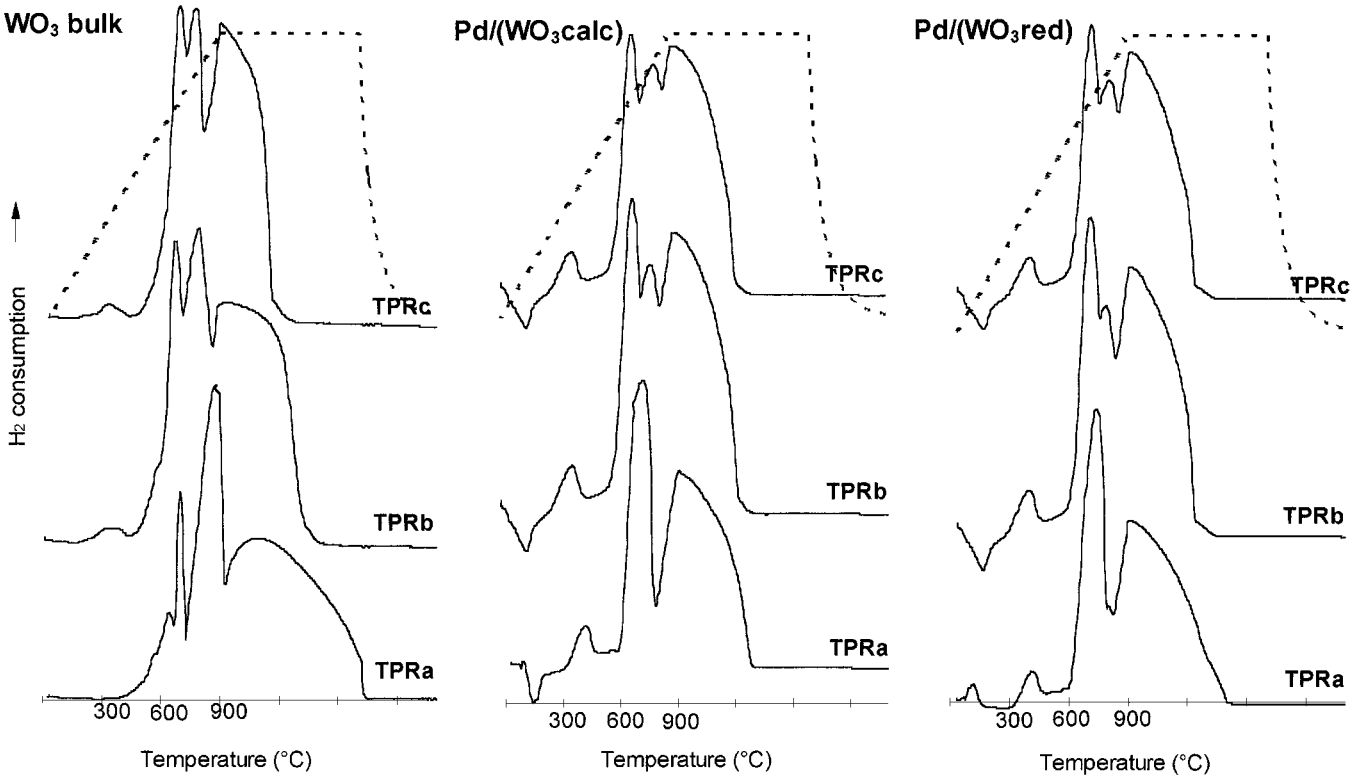

FIG. 1. TPR profiles for WO_3 bulk, Pd/(WO_3calc), and Pd/(WO_3red) obtained for three successive TPR.

Pd/WO_3 catalysts were slightly different initially. The TPRa profile of Pd/(WO_3calc) showed two major peaks at 726 and 900°C and a very weak peak at 429°C. In the case of Pd/(WO_3red), the peaks were observed at 405, 717, and 900°C and a new contribution at 824°C appeared. After reoxidation (TPRb and TPRc), both Pd/WO_3 samples exhibited similar profiles composed of three major consumption peaks but slight differences seemed to remain. Indeed, in the case of Pd/(WO_3calc), no characteristic modification of the peak position was observed whereas Pd/(WO_3red) profiles showed a decrease of the maximum contribution temperature from 757 to 726°C. The total hydrogen consumption was 2.7 ± 0.1 whatever the TPR, which shows a good reproducibility.

TABLE 3

H_2 Consumption for TPR Experiments as a Function of Catalysts

Samples	Step	VH_2 (mol/g)	H_2/WO_x[a]
WO_3	TPRa	$11.7\ 10^{-3}$	2.7
	TPRb	$8.7\ 10^{-3}$	2.0
	TPRc	$6.3\ 10^{-3}$	1.5
Pd/(WO_3calc)	TPRa	$11.9\ 10^{-3}$	2.8
	TPRb	$11.6\ 10^{-3}$	2.7
	TPRc	$12.1\ 10^{-3}$	2.8
Pd/(WO_3red)	TPRa	$11.9\ 10^{-3}$	2.8
	TPRb	$11.5\ 10^{-3}$	2.7
	TPRc	$11.3\ 10^{-3}$	2.6
WO_2	TPRa	$6.3\ 10^{-3}$	1.4
	TPRb	$3.9\ 10^{-3}$	0.8
	TPRc	$1.2\ 10^{-3}$	0.26
Pd/(WO_2red)	TPRa	$8.9\ 10^{-3}$	1.9
	TPRb	$9.9\ 10^{-3}$	2.2
	TPRc	$9.1\ 10^{-3}$	2.0

[a] $WO_x = WO_3$ for WO_3 bulk, Pd/(WO_3calc), and Pd/(WO_3red) and $WO_x = WO_2$ for WO_2 bulk and Pd/(WO_2red).

In the TPR profiles of WO_2 (Fig. 2) three peaks were detected at 628, 715, and 900°C. The total hydrogen consumption (H_2/WO_2) was lower than 2 and decreased to 0.8 and 0.26 after the two reoxidations which were accompanied by a great enhancement of the contribution at 727°C. This means that the reduction of WO_2 into metallic W is more difficult than that of WO_3 and after reoxidation it is still more difficult to reduce. When palladium was added a main peak was observed at 900°C and a smaller one at 739°C on the TPRa (Fig. 2). After reoxidation TPR patterns were better defined and exhibited two maxima at 723 and 900°C. From the profile we can also surmise a contribution at 750°C. As in the case of Pd/WO_3 catalysts, a small contribution at 405°C appeared. These profiles became similar to Pd/WO_3 catalysts with a difference of the hydrogen consumption for the contribution which appears before the consumption at 900°C. The initial total hydrogen consumption was 1.9, which means that nearly all the WO_2 was

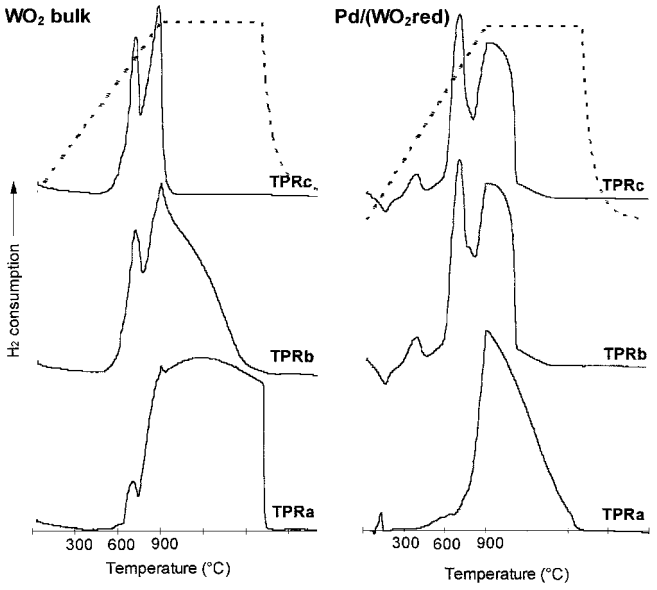

FIG. 2. TPR profiles for WO_2 bulk and Pd/(WO_2red) obtained for three successive TPR.

reduced into metallic W. After reoxidation the hydrogen consumption was still higher (2.3 and 2.1), which suggests the formation of some WO_3. As in the case of Pd/WO_3 catalysts, a H_2 consumption around 400°C was observed. The comparison between WO_2 and Pd/WO_2 clearly shows that palladium helps WO_2 to be reduced but it also helps the reoxidation.

We can note that in most patterns the H_2 consumption at 900°C was dissymetrical. All patterns of palladium-based catalysts showed a small positive peak at 112°C (Pd/(WO_3red)) and 137°C (Pd/(WO_2red)) or a negative contribution at 159°C (Pd/(WO_3calc)) and 173°C (Pd/(WO_3red) and Pd/(WO_2red)) which did not exist for bulk oxides.

3.3. XRD

The various diffraction patterns obtained on all three samples are given in Fig. 3 and the different phases observed are summarized in Table 4. The reduction treatments, LTR and HTR, were performed in a different apparatus for 15 h. A well-identified $W_{20}O_{58}$ phase was evidenced on both Pd/WO_3 samples after reduction at 350°C. It is worthwhile mentioning that during the reduction, Pd/(WO_3red) and Pd/(WO_3calc) samples changed from green and yellow, respectively, to a deep purple colour. The $W_{20}O_{58}$ phase coexists with $W_{24}O_{49}$ after high temperature reduction followed by oxidation and low temperature reduction. A treatment under $[O_2 + H_2O + N_2]$ mixture at 350°C for 4 h after HTR did not modify the bulk oxide $W_{20}O_{58}$. No WO_2 phase was found whatever the reduction temperature on both Pd/WO_3 samples. No new phase was detected on Pd/WO_2 after reduction at 350°C.

TABLE 4

Identified Phases on Pd/(WO_3calc), Pd/(WO_3red), and Pd/(WO_2red) after Various Treatments

Catalysts	Treatments	Identified phases
Pd/(WO_3calc)	As prepared	WO_3
	LTR	$W_{20}O_{58}$
	HTR	α-W
Pd/(WO_3red)	As prepared	WO_3
	LTR	$W_{20}O_{58}$
	HTR	α-W and $W_{20}O_{58}$ (weak)
	LTR + O400 + LTR	$W_{20}O_{58}$
	LTR + $[O_2 + H_2O + N_2]$ for 4 h	$W_{20}O_{58}$
	HTR + O400 + LTR	$W_{20}O_{58}$ and $W_{24}O_{68}$
Pd/(WO_2red)	As prepared	WO_2
	LTR	WO_2
	HTR	α-W

Reduction at 600°C resulted in the formation of α-W on all three samples but $W_{20}O_{58}$ was still detected on Pd/(WO_3red).

3.4. XAS

The intensity and the energy of the W L_{III} edge obtained for each sample as a function of various treatments are reported in Table 5. The W L_{III} absorption edges of Pd/(WO_3red) are shown in Fig. 4. The white line of the catalyst "as prepared" was a little smaller than in the reference WO_3 (Fig. 4). Hydrogen at room temperature decreased the white line peak further, which can be attributed to the formation of a bronze structure H_xWO_3. No modification

TABLE 5

Energy and Intensity of the L_{III} White Lines Pd/(WO_3red) and Pd/(WO_2red) Catalyst as a Function of Various Treatments

Catalysts	Treatments	Energy (eV) (±0.2 eV.)	Normalized intensities $(I_0 - I)/I_0$
References	WO_3	10217.4	2.9
	WO_2	10217.6	1.7
Pd/(WO_3red)	As prepared	10216.9	2.54
	H_2 at 25°C	10217.1	2.41
	LTR	10215.0	2.40
	LTR + HC for 1 h	10216.3	2.41
	LTR + $[O_2 + H_2O + N_2]$ at 350°C for 3 h	10213.8	2.44
	HTR[a]	10216.7	2.24
Pd/(WO_2red)	As prepared	10214.2	1.91
	LTR	10213.6	1.80
	LTR + $[O_2 + H_2O + N_2]$ at 350°C for 5 h	10214.6	1.95
	HTR	10213.5	1.83
	HTR + $[O_2 + H_2O + N_2]$ at 600°C for 3 h	10215.0	2.47

[a] Reduction under H_2 at 500°C for 3 h.

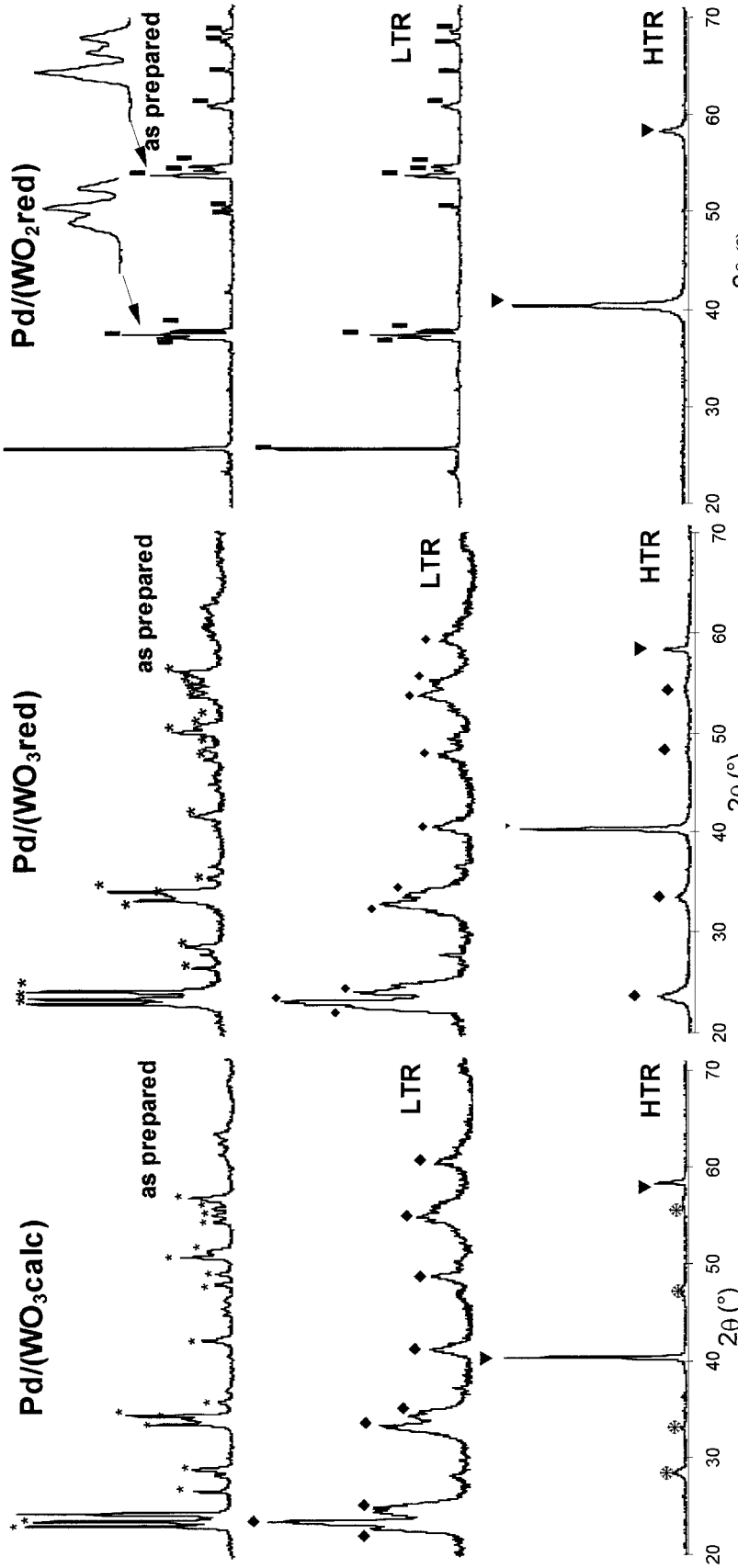

FIG. 3. X-ray diffraction patterns of $Pd/(WO_3calc)$, $Pd/(WO_3red)$, and $Pd/(WO_2red)$ catalysts as a function of reduction treatments, (❋) WO_3 (JCPDS no. 5-0363), (◆) $W_{20}O_{58}$ (JCPDS no. 30-1387), (■) WO_2 (JCPDS no. 32-1393), (▼) α-W (JCPDS no. 4-0806), (❋) Si (JCPDS no. 26-1481). Si is due to a contamination by the quartz reactor.

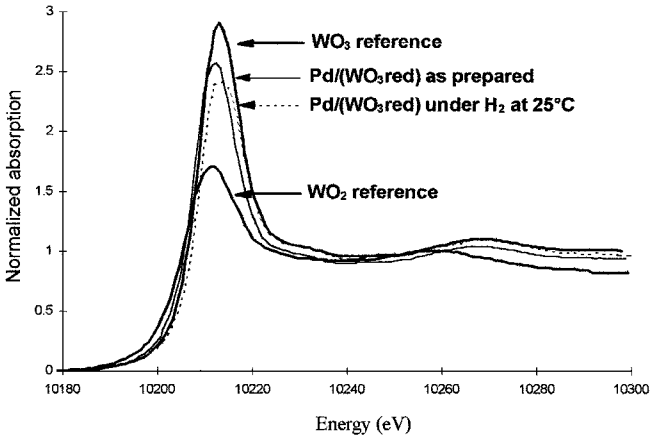

FIG. 4. Normalized *in situ* X-ray absorption spectra of the W L_{III}-edge in Pd/(WO_3red).

took place after reduction under hydrogen for 5 h at 350°C or a mixture of HC/H_2 at the same temperature or even after reduction under hydrogen for 3 h at 500°C. The intensity of the white line of the reference spectrum WO_2 was smaller which means that in all our experiments tungsten was in a $WO_{3-x\ (x<1)}$ state.

Similar studies were performed on Pd/(WO_2red). The intensity of the white line before any treatment was somewhat higher than that of the WO_2 reference compound (Fig. 5A). It decreased with reduction under hydrogen at 350°C but without reaching the peak due to WO_2. It increased again with [$O_2 + H_2O + N_2$] which indicates that an oxidation was taking place. Reduction at 600°C led to a shape, a position in intensity, and energy very close to the metal reference (Fig. 5B). Strong oxidation took place after treatment under [$O_2 + H_2O + N_2$], without reaching, however, the intensity of WO_3.

TABLE 6

Relative Composition for Some Selected Tungsten Compounds as Given by the Literature

Compounds	% W^{6+}	% W^{5+}	% W^{4+}	References
$W_{20}O_{58}$	Present	Present	Present	(40)
	72	28	Detected	(41)
	80	20	0	(45, 46)
	75	25	0	(47, 48)
$W_{18}O_{49}$	56	32	12	(41)
	71	29	0	(45)
	71	15	14	(46)
$H_{0.35}WO_3$	84	16	0	(44, 49)
$H_{0.50}WO_3$	47	30	23	(32)

3.5. *XPS*

Various oxidation states of W have been identified in many XPS studies (13–15, 32–49). Reduction of WO_3 can lead to W^{5+}, W^{4+}, and W^0 while W^{2+} is rather doubtful. W^{6+} and W^{4+} correspond to well-defined oxides while W^{5+} can hardly be attributed to W_2O_5. Several stable phases, $W_{20}O_{58}$, $W_{18}O_{49}$ or hydrogen bronzes H_xWO_3 are a mixture of different oxidation states in proportions which are reasonably well established in the literature (see Table 6). The binding energies (E_b) corresponding to the various oxidation states vary noticeably in the literature, depending on the energy reference. Following previous studies (13, 14) we chose the following values for the W $4f_{7/2}$ transition: $W^{6+} = 35.6 \pm 0.1$ eV, $W^{5+} = 33.9–34.5$ eV, $W^{4+} = 32.9 \pm 0.1$ eV, $W^0 = 31.2 \pm 0.1$ eV. The relative inaccuracy in W^{5+} is due to the fact that no pure and stable reference was available in that case.

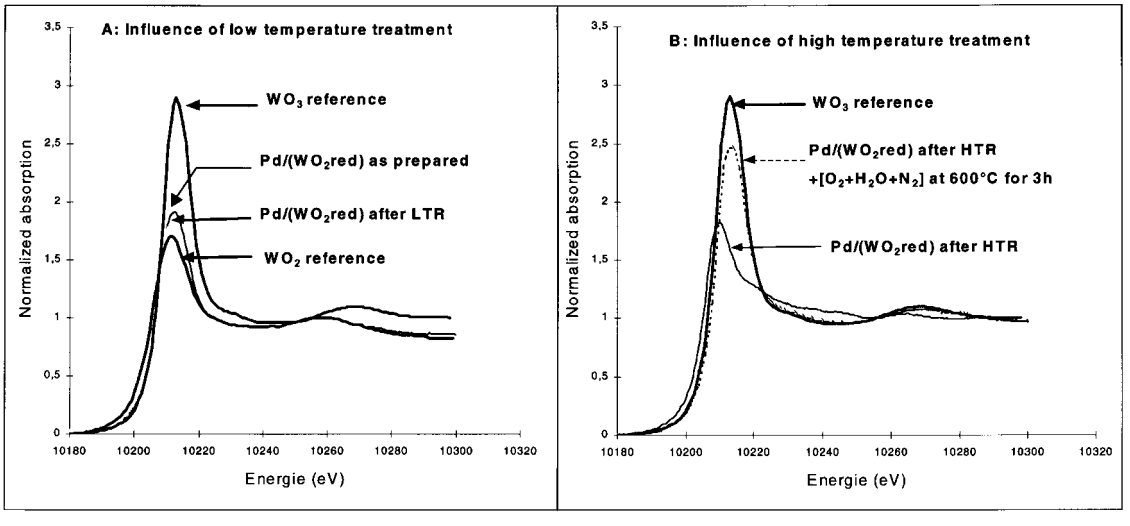

FIG. 5. Normalized *in situ* X-ray absorption spectra of the W L_{III}-edge in Pd/(WO_2red) catalyst.

TABLE 7

Relative Concentrations of Different States of Tungsten and Atomic Pd/W Ratios as a Function of Various Treatments for Pd/(WO_3red)

Samples	Relative concentrations of different states of tungsten (%)				Ratio	Atomic
	W^{6+}	W^{5+}	W^{4+}	W^{o}	W^{5+}/W^{6+}	Pd/W ratio
As prepared	100	0	0	0	—	0.041
R350/4 h	64	36	0	0	0.56	0.033
R350/8 h	63	36	0	Traces	0.56	0.039
R350/12 h	63	36	0	Traces	0.56	0.041
O400/1 h[a]	100	0	0	0	—	0.027
R350/4 h[b]	65	35	0	0	0.54	0.036
R600/1 h[c]	12	11	0	77	0.92	0.039
R600/4 h	12	7	0	81	0.58	0.043
R600/8 h	9	7	0	84	0.78	0.080

[a] 12-h reduction at 350°C followed by 1-h oxidation under air.
[b] Same as above but followed by a new 4-h reduction.
[c] Experiment performed on an "as prepared" sample.

Pd/(WO_3red). Table 7 gives the percentages of the different oxidation states derived from curve fitting analysis of W 4*f* peaks recorded after various treatments. In Fig. 6 we show a few typical spectra. Reduction at 350°C (R350) led to W^{5+} in addition to W^{6+} and prolonged exposures to hydrogen gave identical results apart from minute amounts of metallic W. Here again, the sample turned to a blue–purple colour. It must be emphasized that no or very little W^{4+} oxidation state, corresponding to the oxide WO_2, was found during these reduction studies. The formation of W^{5+} can be attributed either to a bronze or to an oxide $W_{20}O_{58}$ or $W_{18}O_{49}$. However the W^{6+}/W^{5+} ratios and the absence of W^{4+} suggest that $W_{20}O_{58}$ was actually formed in agreement with X-ray diffraction studies. Reduction at higher temperature (R600) leads to a majority of W metal; nevertheless, some W^{6+} and W^{5+} remained.

The Pd 3*d* peaks were also recorded. All the reductions led to 100% metallic palladium ($E_b = 335.1$ eV) and oxidation at 400°C gave PdO ($E_b = 337.0$ eV), as expected. However, a surprising result was the presence of 87% metallic palladium initially. It must be remembered that the support was reduced but no further reduction was performed after impregnation: the catalyst was only dried. The Pd/W ratio (atomic) was 0.04 initially (see Table 7), which means that palladium was well dispersed on the support. It did not change very much during the reductions, with, however, a tendency to increase at higher temperature. Chlorine ($E_l = 198.7$ eV) was detected on the fresh sample only (Cl/Pd = 2.6) and disappeared after the first reduction.

Pd/(WO_3calc). Some W^{5+} was observed in the initial spectrum obtained before the calcination of the catalyst during the preparation. It disappeared after calcination was

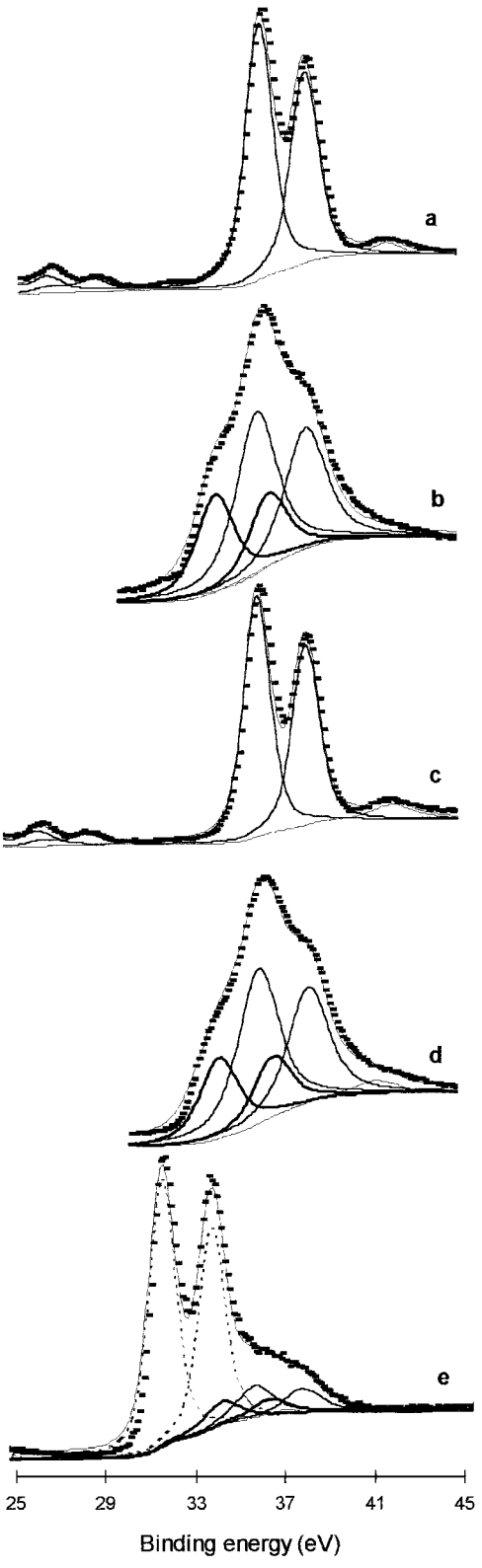

FIG. 6. Changes in W4*f* lines as a function of various treatments for Pd/(WO_3red) catalyst as prepared (a), 4 h reduced at 350°C, (b), 12 h reduced at 350°C (R350) followed by a 1 h oxidation at 400°C (O400) (c), sample c reduced 4 h at 350°C (d) and Pd/(WO_3red) "as prepared" reduced 1 h at 600°C (e).

TABLE 8

Relative Concentrations of Different States of Tungsten and Atomic Pd/W Ratios as a Function of Various Treatments for Pd/(WO_3calc)

Samples	Relative concentrations of different states of tungsten (%)				Ratio	Atomic
	W^{6+}	W^{5+}	W^{4+}	W°	W^{5+}/W^{6+}	Pd/W ratio
Before calcination	83	17	0	0	0.20	0.13
As prepared	100	0	0	0	—	0.08
R350/4 h	48	27	0	25	0.56	0.03
R350/8 h	32	18	0	50	0.56	0.04
R350/12 h	7	3	0	90	0.43	0.04
R600/1 h[a]	≤5	≤5	0	95	0.25	0.04
R600/4 h	0	0	0	100	—	1.00

[a] Experiment performed on an "as prepared" sample.

performed at 400°C leading to the "as prepared catalyst". All subsequent reductions were performed on the latter surface. Unlike the previous sample, low temperature reduction resulted in the formation of metallic W (Table 8 and Fig. 7), which increased as a function of time. After 12 h at 350°C, the surface was almost completely reduced. No oxide at all was detected after 4 h at 600°C. Again no W^{4+} was detected and the ratio W^{5+}/W^{6+} (0.56) found in the initial stages of the low temperature reduction was the same as with Pd/(WO_3red); $W_{20}O_{58}$ was therefore probably present although W^{5+}/W^{6+} was somewhat higher than expected.

Some metallic palladium (28%) was present initially, but in a smaller amount than in the previous sample. Reduction gave 100% Pd. Chlorine was detected only on the "as prepared" sample but in too small an amount to be quantified. The initial Pd/W ratio, 0.13, was very high. It decreased after reduction. It was only 0.04 after the reduction treatment at 350°C. However reduction for 4 h at 600°C resulted in equal amounts of Pd and W on the surface. This result can probably be interpreted as due to the formation of an alloy Pd_xW_y.

Pd/(WO_2red). The surface of WO_2 is easily oxidized in the open air. It is the reason why 85% of W^{6+} was detected on the initial compound (Table 9). It is not very deeply oxidized though, since some WO_2 was still present in the spectrum. If one remembers that the binding energy of W 4*f* peaks is very low (around 30 eV) and therefore the kinetic energy of the emitted photoelectrons is about 1450 eV, which corresponds to an inelastic mean free path λ of 1.75 nm, following Powell and colleagues (64), one can easily calculate that the thickness of the WO_3 contamination was about 2λ, that is, 3.5 nm. Reduction at 350°C as a function of time resulted in a slow increase of metallic W but even after 16 h under hydrogen the sum $W^{5+} + W^{6+}$ was still 40% (Figs. 8 and 9 and Table 9). The different values of the ratio W^{5+}/W^{6+} correspond to a surface more oxygen

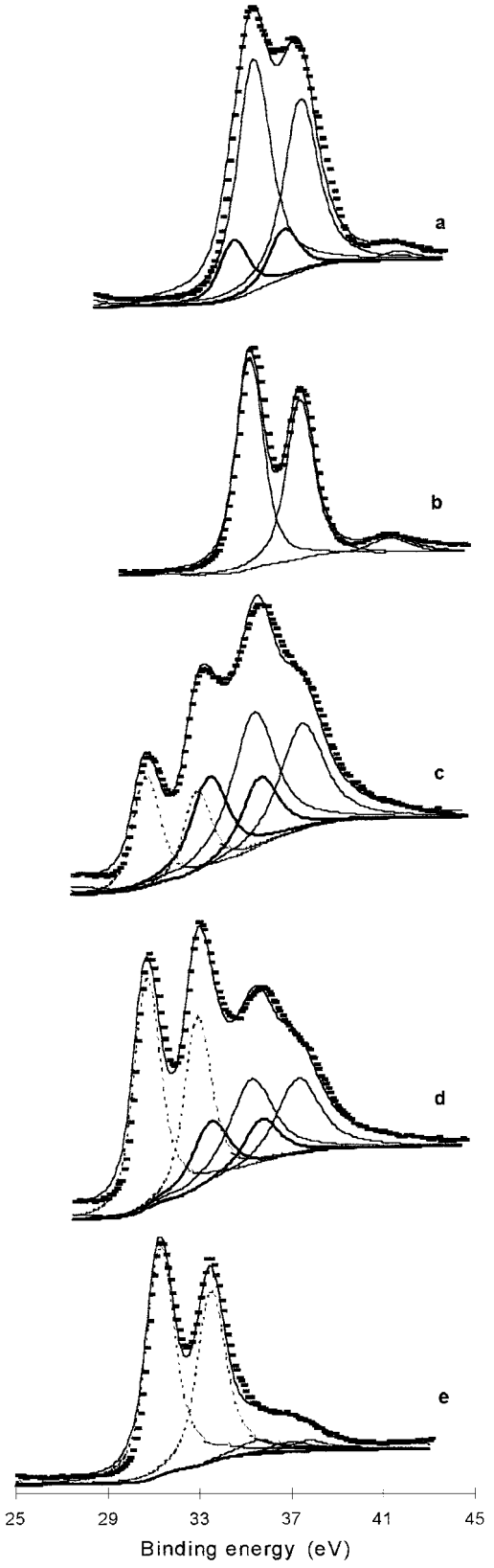

FIG. 7. Changes in W4*f* lines as a function of various treatments for Pd/(WO_3calc) catalyst before calcination (a), "as prepared" (b), 4 h reduced at 350°C (c), 8 h reduced at 350°C (d), 12 h reduced at 350°C (e).

deficient than the well-defined $W_{20}O_{58}$ phase. Metallic W and WO_2 were no longer detected after reoxidation at 400°C but pure WO_3 was not found since 33% of W^{5+} was present, which suggests the formation of $W_{20}O_{58}$. Reduction at 600°C allowed the reduction of the superficial oxidized skin (WO_x and $x > 2$) into metallic W without concerning the WO_2 substrate.

After another reduction at 350°C for 15 h, giving exactly the same composition as for 16 h at 350°C in 4 h steps, we treated the sample at 350°C under the $[O_2 + H_2O + N_2]$ mixture. Complete oxidation into WO_3 took place, within the detection depth of the technique. A new reduction for 15 h at 350°C had very little effect since 77% of WO_3 was still detected. Never again would W metal be detected. Heating under vacuum for 1 h at 350°C resulted in little further reduction.

Palladium initially was largely reduced: 67% of metallic Pd was observed. Pd/W ratios were quite high: 0.44 initially, which is probably due to the very low surface area of this sample, as compared with the two Pd/WO_3 catalysts. However, the ratio decreased significantly after reduction, especially at high temperature, down to 0.09 after 8 h at 600°C. Chlorine was initially present (Cl/Pd = 2.9) but was no longer detected.

TABLE 9

Relative Concentrations of Different States of Tungsten and Atomic Pd/W Ratios as a Function of Various Treatments for Pd/(WO_2red)

Samples	Relative concentrations of different states of tungsten (%)				Ratio	Atomic
	W^{6+}	W^{5+}	W^{4+}	W°	W^{5+}/W^{6+}	Pd/W ratio
As prepared	85	0	15	0	—	0.44
R350/4 h	54	19	27	0	0.35	0.37
R350/8 h	19	18	43	19	1.00	0.24
R350/12 h	20	23	35	22	0.87	0.30
R350/16 h	17	23	32	28	0.73	0.27
O400/1 h[a]	67	33	0	0	0.49	0.05
R350/4 h[b]	65	24	11	0	0.37	0.08
R600/1 h[c]	5	13	25	57	0.38	0.20
R600/4 h	0	0	13	87	—	0.10
R600/8 h	0	0	12	88	—	0.09
R350/15 h[c]	25	18	26	31	1.40	0.20
$[O_2 + H_2O + N_2]$/4 h[d]	100	0	0	0	—	0.07
R350/15 h[e]	77	16	5	0	0.20	0.08
Vacuum 350/1 h[f]	68	20	7	5	0.29	0.02

[a] 16-h reduction at 350°C followed by 1-h oxidation under air.
[b] Same as above but followed by a new 4-h reduction.
[c] Experiment performed on an "as prepared" sample.
[d] 15-h reduction at 350°C without analysis step followed by a 4-h treatment under a $[O_2 + H_2O + N_2]$ mixture.
[e] Same as above but followed by a new 15-h reduction at 350°C.
[f] Same as above but followed by a 1-h treatment under vacuum at 350°C.

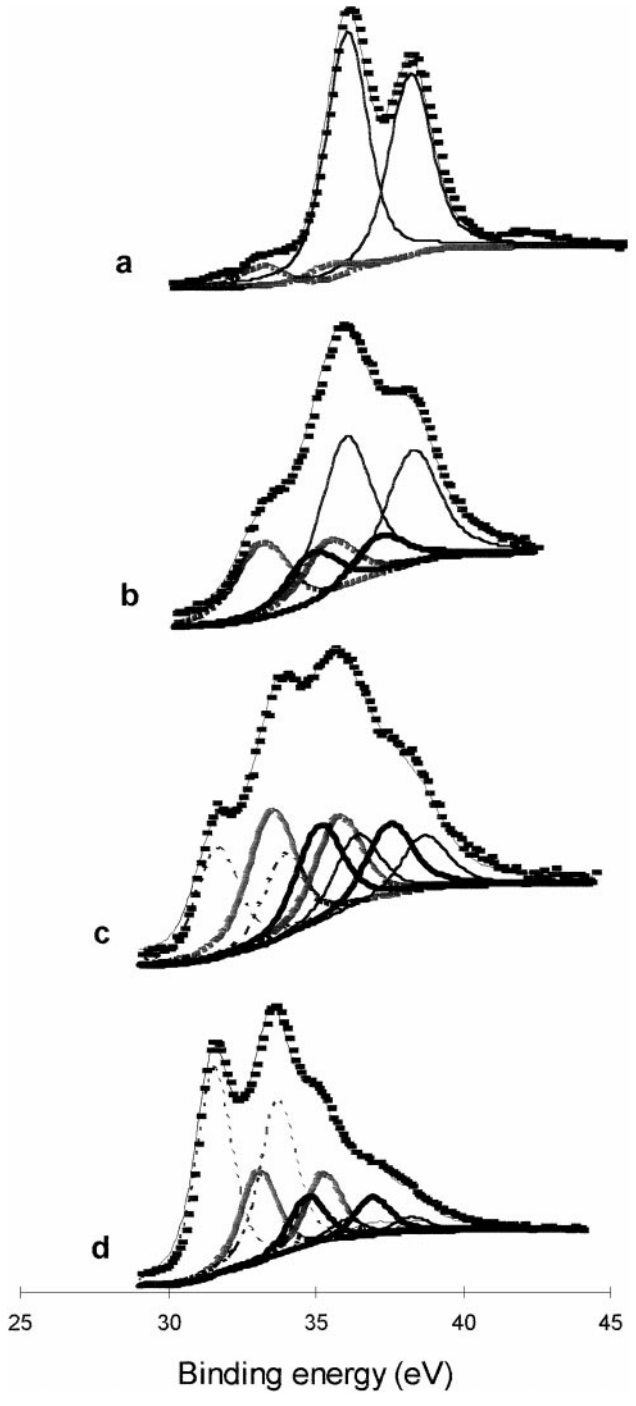

FIG. 8. Changes in W4*f* lines as a function of reduction treatments for Pd/(WO_2red) catalyst: "as prepared" (a), 4 h reduced at 350°C (b), 8 h reduced at 350°C (c), 1 h reduced at 600°C (d).

4. DISCUSSION

A striking result of our experiments is that reduction under hydrogen at 350 and 600°C of Pd/WO_3 (Pd/(WO_3calc) and Pd/(WO_3red)) does not lead to the formation of WO_2

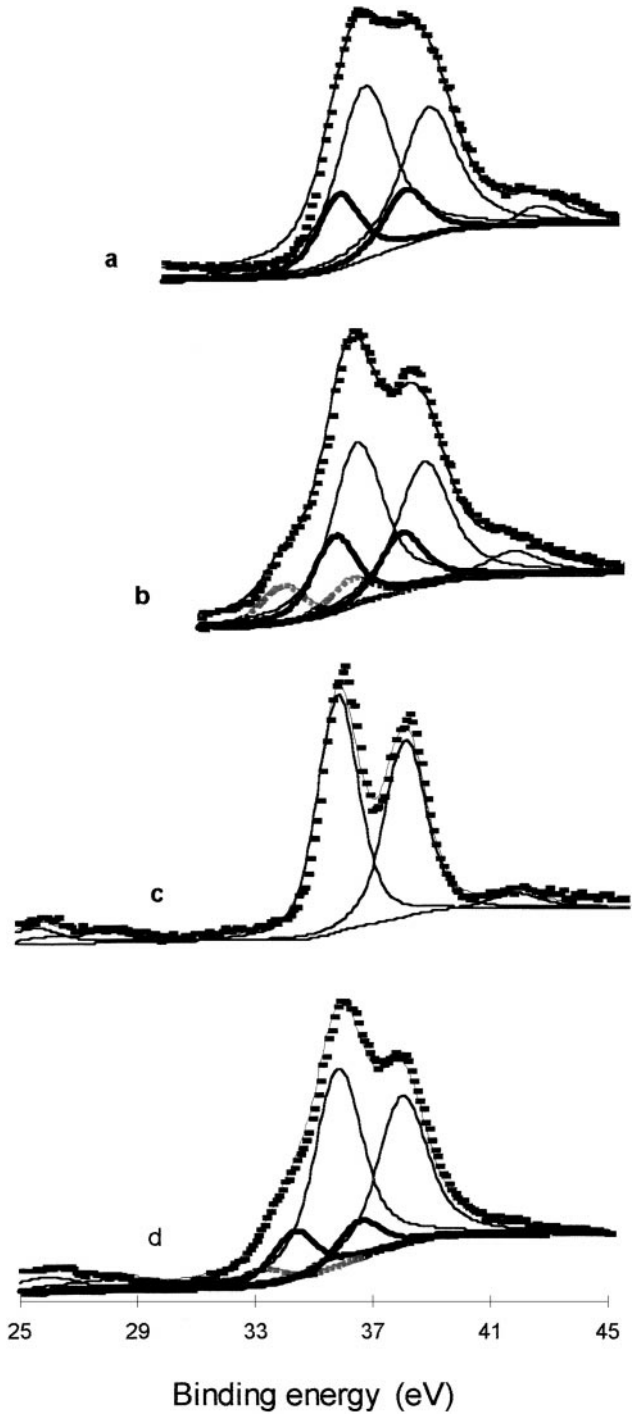

FIG. 9. Changes in W4*f* lines as a function of various treatments for Pd/(WO_2red) catalyst. Influence of an oxidation treatment under air for 1 h at 400°C (a) followed by a new reduction at 350°C for 4 h (b) and under [$O_2 + H_2O + N_2$] mixture for 4 h at 350°C on catalyst prereduced *in situ* at 350°C for 15 h (c) followed by a new reduction for 15 h (d).

or if it does, very small amounts are detected. Bulk and surface techniques are very consistent in that respect.

X-ray diffraction studies showed that the reduction is not a surface process only and that the bulk is also modified. After low temperature reduction of both Pd/WO_3 samples a single, $W_{20}O_{58}$, phase was detected. High temperature reduction led to metallic α-W with some residual $W_{20}O_{58}$. Reoxidation followed by reduction at 350°C gave another phase, $W_{24}O_{68}$, together with $W_{20}O_{58}$. The former was identified by Hoang-Van and Zegaoui after reduction of 0.2% Pt/WO_3 17 h at 300°C (22). $W_{20}O_{58}$ was also observed on WO_3 reduced under hydrogen 5 h at 400°C (48). No intermediate phase was observed when WO_2 was reduced into metallic W.

TPR experiments showed that on all samples, with or without palladium, the reduction is a multistep process. From hydrogen consumption measurements it can be concluded that WO_3 bulk is easier to reduce into metallic W ($H_2/WO_3 = 2.7$) than WO_2 bulk since after the first TPR, $H_2/WO_2 = 1.4$ only and the latter ratio decreased drastically after the second and the third experiment, indicating that after reoxidation WO_2 is even more difficult to reduce.

The reduction of WO_3 and WO_2 has been largely studied by TPR and thermogravimetric analysis (12, 50–56). The attribution of the different peaks to specific species is not easy because the temperatures observed depend largely on the experimental conditions. Vermaire and Van Berge (50) showed that the reduction temperatures of the different reduction steps depend largely on the weight of catalyst as confirmed by Fouad *et al.* (56). As pointed out by Sahle and Berglund (57) these discrepancies are probably due to the kinetics of the evolution of water formed during the reduction process, which depends on the hydrogen flux, the height of the catalyst bed, and the rate of the temperature increase. Similar explanations were given by Arnoldy *et al.* (58) for MoO_3 and MoO_2 reduction. The water vapour formed during the initial stage will influence the further course of reduction. Indeed, several authors (57–59) showed that the gradient of water vapour determined the formation of intermediate phases. For example, it has been reported that a certain minimum of humidity would be necessary for the formation of the $WO_{2.72}$ phase (59, 60). These considerations explain the large and dissymetrical peak at 900°C attributed to the reduction of WO_2 in W^0. From the thermodynamic point of view, this limitation of reduction is understandable because calculations have demonstrated that the reduction of WO_2 has a small equilibrium constant as pointed out by Sahle (57). Schubert studied in detail the WO_3 reduction with kinetic and morphological considerations (59). This author illustrated the reaction scheme of tungsten reduction which clearly summarized the different possible steps as a function of the temperature (Fig. 10). On this basis and our observations (XRD and XPS) we can tentatively attribute the various peaks observed in our experiments:

$$WO_3 \rightarrow WO_x \ (W_{20}O_{58} \text{ at } 572^\circ\text{C}, W_{18}O_{49} \text{ at } 635^\circ\text{C}, W_{24}O_{68} \text{ at } 707^\circ\text{C})$$

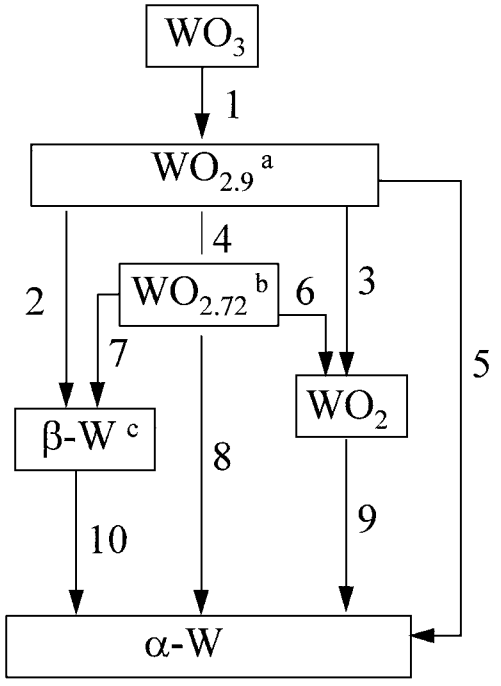

FIG. 10. Reaction scheme of tungsten oxide reduction by Schubert (59) (a) $WO_{2.9} = W_{20}O_{58}$; (b) $WO_{2.72} = W_{18}O_{49}$; (c) β-W = W_3O.

$$WO_3, WO_x \rightarrow WO_2 \ (752\text{–}871^\circ C)$$
$$WO_2 \rightarrow W^0 \ (900 \text{ and } > 900^\circ C)$$

These attributions agree with the results of Vaudagna *et al.* (29). The different reduction peaks of WO_3 in the TPR were attributed to $WO_3 \rightarrow WO_{2.9}$ (shoulder at about 620°C), WO_3 and $WO_{2.9} \rightarrow WO_2$ (maximum at 793°C), and $WO_2 \rightarrow W^0$ (last peak).

On WO_2 the peak at lower temperature (715°C) is probably due to the reduction of superficial WO_3. As previously shown (13) and confirmed by the present paper, the first layers of WO_2 are largely composed of WO_3 and reoxidation at 400°C, as shown by XPS, proceeds even deeper, which explains why the TPR peak at 715°C is higher in the second and third TPR (Fig. 2).

The TPR patterns of palladium-based catalysts are similar to those observed for bulk oxides and show that the reduction proceeds through similar stages even if their contributions seem to be modified. The contribution at 900°C is also dissymetrical. The water vapour evolved during the reduction is always a limitant factor even in the presence of palladium. Hovewer, the addition of palladium leads to a stabilization of the hydrogen consumption: after all three TPR experiments on both Pd/WO_3 and Pd/WO_2 the overall hydrogen consumption values were close to 3 and 2, respectively, which suggests that palladium catalyzes oxidation and high temperature reduction processes. Similar conclusions were previously derived from studies with Pd or Pt on WO_3 or MoO_3 (19, 25–29). The authors explained these phenomena with a hydrogen spillover effect: hydrogen dissociated on the metal will be able to migrate on the support, facilitating its reduction. The small positive peaks at low temperature (112–137°C) for Pd/(WO_3red) and Pd/(WO_2red) obtained on the first TPR (Figs. 1 and 2) are certainly due to the reduction of palladium salt $Pd(NH_3)_4Cl_2$ or a decomposed type of this salt $PdCl_2$. A tentative calculation of the hydrogen consumption H/Pd gives, respectively, 0.48 and 0.39, which are smaller values than expected for the total reduction of palladium. Hovewer, it is reasonable to ascribe these consumptions to the reduction of the Pd salt and it is consistent with our XPS results which show that a high quantity of palladium is already in its metallic state on the surface before any reduction. After an oxidation treatment, all the palladium would be in the oxidized state PdO. This species would be reduced at a temperature lower than ambient temperature, which could not be observed in our apparatus. Other TPR results obtained for Pd–3%/WO_3–Al_2O_3 or free Al_2O_3 catalysts, showing PdO reduction at 8°C, confirmed this idea (17). Hence, the negative contribution around 160°C for the next TPR could be due to the decomposition of palladium hydride formed at low temperature. Our proposals agree with the results of Juan *et al.* (19) who observed the decomposition of palladium hydride above 100°C for Pd/MoO_3 catalysts. They specified that "severe oxidation treatment" is required to turn Pd "visible" by TPR. This explains why only a negative peak was observed in the case of Pd/(WO_3calc) for which both the support and the catalyst were calcined leading to PdO. Here again this explanation agrees with XPS results showing only traces of chlorine and confirms that palladium is not in a "chlorine palladium" form.

It seems difficult to attribute the contribution at 400°C to the palladium presence. Indeed, this contribution is observed in many cases except for bulk WO_2, and such a temperature of reduction was never reported for palladium. So it could be attributed to the reduction of a small quantity of WO_3 due to an interaction between palladium and the oxide, via a spillover process, leading to a partial reduction of the oxide at a temperature lower than in the absence of transition metal as proposed by several authors (17, 25, 28, 32). An alternative explanation would be the formation and decomposition of a tungsten bronze (HTB), as suggested by Bond and Tripathi (27). These authors have reported for a 1% Pd/WO_3 catalyst that the reduction of WO_3 began at 230°C leading to 377°C to the W_4O_{11} oxide (currently attributed to $W_{18}O_{49}$). They speculated that a HTB formed at 50°C reacted with the lattice oxygens to form the W_4O_{11} phase. This interpretation could explain our present results. Indeed, the contribution is smaller in the case of bulk WO_3 which was probably due to the difficulty of obtaining atomic hydrogen on oxides. Consequently, the HTB's percentage would be more important for Pd/WO_2 and Pd/WO_3 catalysts and the decomposition into WO_x phase also. The

different steps could be summarized as:

(1) dissociation of hydrogen on Pd: $H_2 \rightarrow 2H^*$
(2) formation of bronze: $xH^* + WO_3 \rightarrow HxWO_3$
(3) decomposition under heating leading to a non stoichiometric oxide: $2H_xWO_3 \rightarrow 2WO_{3-(x/2)} + xH_2O$.

The results reported by Regalbuto *et al.* corroborate this hypothesis (32). To explain that Pt facilitates the partial reduction of the supported tungsta ($Pt/WO_3/SiO_2$) catalyst, the existence of very thin layers of HTB stabilized by the metal was postulated. The authors invoked the elimination of hydrogen as water resulting in anhydrous suboxides formation with compositions in the $WO_{2.7}$–$WO_{2.84}$ range.

Qualitative results obtained by XAS on Pd/WO_3 and Pd/WO_2 confirm that hydrogen treatments at 350°C lead to a moderate reduction of the oxide; that is, the composition WO_2 is not attained. It is likely that $W_{20}O_{58}$, where W atoms stay in their octahedral environment, is present rather than $W_{18}O_{49}$ since in the latter case a pentagonal bipyramid would be formed and the shape of the spectrum would be much more modified than actually observed (61, 62). This hypothesis is consistent with the XRD results. On WO_2 hydrogen treatment at 350°C resulted in a very weak reduction, probably of the superficial WO_3, while at 600°C metallic W was formed.

Surface analyses by XPS largely confirmed these findings. In particular curve fittings of the spectra obtained after reduction of Pd/WO_3 at 350°C failed to reveal the presence of W^{4+}: trying to introduce such a species in the analysis led either to erroneous binding energies or to contributions which were much too narrow, as compared with reference spectra. This is consistent with previous results obtained on WO_3 after reduction under hydrogen at 350°C (15).

From the XPS results we can compare the reducibility of the three catalysts after the hydrogen treatment at 350°C. When the WO_3 support was reduced ($Pd/(WO_3red)$) oxidation states +6 and +5 only were detected. A good stability of the surface was obtained after 4 h under hydrogen and it was fairly reproducible after an oxidation–reduction cycle, which seems to be related to the formation of a $W_{20}O_{58}$ phase, detected by XRD. Hovewer the W^{5+}/W^{6+} ratio is slightly higher (0.43–0.56) than the value reported by several authors for bulk oxides (41, 43, 45–48). We believe that this phenomenon can be attributed to the presence of the metal. Similar ratios have been obtained on $Pd/WO_3/Al_2O_3$ reduced at 200°C and $Pt/WO_3/SiO_2$ reduced at 400°C (17, 32). An interesting result was obtained by Gehlig *et al.* (45) who studied the influence of metallic dopants such as V, Ni, and Nb on the state of $WO_{2.90}$ and $WO_{2.72}$ W4*f* levels. The main effect was an increase in the $W4f^{5+}$ state density with the proportion of dopants. No chemical shift and no modification of the contribution in the filling of the conduction band was observable. So, the authors concluded that a possible explanation was that the dopant lowers the tungsten levels in their vinicity which could favour the conduction band states close to the Fermi level. Calcination of the WO_3 support ($Pd/(WO_3calc)$) had a dramatic effect: after 4 h under hydrogen 25% of W^0 were found and the surface seemed almost completely reduced after 12 h. Metallic tungsten seems therefore to be easily formed in that case although another possibility would be the presence of the so-called β-phase (W_3O), almost impossible to distinguish from metallic tungsten by XPS. β-W was previously identified by XRD for reduced WO_3 bulk and Pt/WO_3 (22, 59). It may be worth mentioning that after 12 h under hydrogen the sample became pyrophoric, which might be an indication for the β-phase. It is worthwhile to recall that even after a long time under H_2, some W^{5+} and W^{6+} remain. So we believe that the $W_{20}O_{58}$ phase is always present in the surface as in the bulk (XRD). The probable presence of W_3O is consistent with the reduction scheme proposed by Schubert (59). Indeed, this phase can be directly formed from $W_{20}O_{58}$. Small quantities of W_3O could accelerate the reduction of tungsten oxide. However, the β-W $\rightarrow$ α-W transformation proceeds very slowly. The reason for such a difference of behaviour between $Pd/(WO_3red)$ and $Pd/(WO_3calc)$ is not straightforward. One may invoke in the latter case a higher concentration of palladium on the surface ($Pd/W = 0.13$ instead of 0.04) which might favour the reducibility. Another possibility would be a strong Pd $\leftrightarrow$ WO_x interaction taking place if the support is reduced before the impregnation.

A stable surface was obtained after 8 h of reduction on Pd/WO_2 ($Pd/(WO_2red)$). It was composed of W^{6+}, W^{5+} (both resulting from the initial superficial oxidation), W^{4+}, and some W^0, the presence of which does not seem to help any further reduction. Although these results are different from Pd/WO_3 samples, it is possible that the reduction proceeds through the same $W_{20}O_{58}$ phase if one considers $Pd/(WO_2red)$ as $Pd/(WO_3)$ supported on WO_2. The W^{4+} species are probably due to the WO_2 underlying layers (bulk). From our XRD and XAS results, we believe that only the WO_3 due to contamination is reduced. Oxidation treatments lead to a hardly reducible surface which could be attributed to a further growth of WO_3 layers. An interaction between the two oxides can also explain the difficulty to reduce WO_2.

High temperature reduction led in all three cases to a majority of metallic tungsten with, however, small amounts of residual oxides.

The percentage of metallic palladium in $Pd/(WO_3red)$ and $Pd/(WO_2red)$ samples was very high (87 and 67%, respectively) even before any hydrogen treatment. It was much lower (28%) when the support was calcined before impregnation. The same observation was showed by electron microscopy for $Pd/WO_3/Al_2O_3$ prepared from $PdCl_2$ and by XPS for $Pt/WO_3/SiO_2$ prepared from H_2PtCl_6 (20, 32). It is interesting to note that these catalysts were

calcined after salt impregnation. Conversely, $Pd/WO_3/Al_2O_3$ catalyst prepared from chlorine free salt ($Pd(NO_3)_2$) did not present this characteristic and 100% of palladium was in the oxide state (17). With regard to these observations, it appears that a metallic precursor containing Cl is necessary to observe such a phenomenon. A thermal decomposition of the metal oxide, as proposed by Vaudagna *et al.* for Pt/ZrO_2 catalysts, seems unlikely (29). Indeed, this catalytic system was calcined at 800°C leading to PtO whereas, in the present study, $Pd/(WO_3red)$ and $Pd/(WO_2red)$ were only dried after impregnation. In our opininon, two suggestions can explain the presence of metallic Pd. The first hypothesis is based on an autoreduction of $Pd(NH_3)_4Cl_2$ according to the reduction scheme (i) or (ii):

scheme (i)
$$Pd(NH_3)_4Cl_2 \rightarrow 2N_2 + 6H_2 + PdCl_2 \quad [1]$$
$$PdCl_2 + H_2 \rightarrow Pd^0 + 2HCl \quad [2]$$
$$Pd(NH_3)_4Cl_2 \rightarrow Pd^0 + 2N_2 + 4H_2 + 2HCl \quad [3] = [1] + [2]$$

scheme (ii)
$$2Pd(NH_3)_4Cl_2 \rightarrow 4N_2 + 12H_2 + 2PdCl_2 \quad [4]$$
$$PdCl_2 + H_2 \rightarrow Pd^0 + 2HCl \quad [2]$$
$$2Pd(NH_3)_4Cl_2 \rightarrow Pd^0 + PdCl_2 + 4N_2 + 10H_2 + 2HCl \quad [5] = [4] + [2]$$

This suggestion could explain that metallic palladium is obtained for all catalysts ($Pd/(WO_3calc)$, $Pd/(WO_3red)$, and $Pd/(WO_2red)$). Hovewer, this proposal does not take into account the differences observed, especially if the support is precalcined or prereduced or it is necessary to imagine that this process is activated in the presence of WO_{3-x}. Such a conclusion is not consistent with large amounts of chlorine found on $Pd/(WO_3red)$ and $Pd/(WO_2red)$ ($Cl/Pd = 2.6$ and 2.85, respectively) while only traces were present on the $Pd/(WO_3calc)$ surface. One must not forget either that tungsten was found in W^{6+} state for $Pd/(WO_3red)$ and $Pd/(WO_2red)$ whereas traces of W^{5+} were observed for $Pd/(WO_3calc)$. These results were in opposite order to what was expected. So we can hardly exclude a role of the support and we propose another explanation based on these observations. Dicko *et al.* (63) suggested a participation of the support to explain the presence of Pt° for $Pt/ZrO_2/SO_4^{2-}$. For $Pd/(WO_3red)$ and $Pd/(WO_2red)$, an oxido-reduction process will be attractive. This suggestion is based on the oxido-reduction potential in solution: $E_1^\circ(Pd^{2+}/Pd^0) = +0.951$ V and $E_2^\circ(WO_3/W_2O_5) = -0.029$ V. W_2O_5 is currently attributed to the $W_{18}O_{49}$ phase, which is close to $W_{20}O_{58}$. The supports were prereduced at 350°C for 15 h and in these conditions, the XPS results let us conclude to the formation of $W_{20}O_{58}$. So it is convenient to consider the E_2° potential. The total reaction is simplified as

$$Pd^{2+} + W_2O_5 + H_2O \rightarrow Pd^0 + 2WO_3 + 2H^+. \quad [6]$$

The residual chlorine could therefore be located on the tungsten oxide "W*x*O*y*Cl," as proposed by Juan *et al.* (19) who suggested volatile oxichloride of molybdenum to explain a transport mechanism.

5. CONCLUSION

In this study we have shown that the bulk and surface properties of Pd/WO_x catalysts depend very much on the chemical state of the oxides before impregnation with the palladium salt. In particular the reducibility of Pd/WO_3 is very different whether the tungsten oxide was previously calcined at 400°C (Pd/WO_3calc) or reduced at 350°C ($Pd/(WO_3red)$). Likewise, the role of the WO_3 contamination layers, covering the WO_2 bulk oxide, was evidenced.

Reduction at moderate temperature of Pd/WO_3 led to the formation of $W_{20}O_{58}$. However, while this phase was stable after 4 h under hydrogen when the WO_3 oxide was reduced before impregnation ($Pd/(WO_3red)$), further reduction occurred, into metallic tungsten or possibly W_3O, if the support was previously calcined ($Pd/(WO_3calc)$). It is important to underline that in neither case was a phase characteristic of W^{4+} (WO_2) detected. In both cases, the initial step of reduction is the formation of the $W_{20}O_{58}$ phase which occurred both on the surface and in the bulk.

Hydrogen on Pd/WO_2 ($Pd/(WO_2red)$) under the same conditions allowed the reduction of most of the superficial WO_3 oxide to $W_{20}O_{58}$ and small amounts of metallic tungsten were also formed, favouring the process of water elimination leading to higher reduction. A stable surface composition was obtained after 8 h under hydrogen in our experimental conditions (weight, flow..). Nevertheless, an oxidation treatment acts as a limitant factor for the reduction and no more W metal was detected. The composition of the surface is also similar to that observed for Pd/WO_3 catalysts.

Prereduction of the WO_3 and WO_2 supports leads to metallic Pd formation without a reduction treatment.

In all three cases, ($Pd/(WO_3calc)$, $Pd/(WO_3red)$, and $Pd/(WO_2red)$), high temperature reduction, at 600°C, led to surfaces composed predominantly of metallic tungsten. We have proposed the formation of the W_3O phase. An alloy may be formed when the support was calcined prior to impregnation.

In a subsequent paper we will try to correlate these findings with the reactivity of these catalysts.

ACKNOWLEDGMENTS

Many thanks are due to Mrs. A. Meens for her help with the XPS measurements and to Dr. R. Revel and Mr. J. L. Schmitt for their participation in the XAS studies.

REFERENCES

1. Grunert, W., Shpiro, E. S., Feldhaus, R., Anders, K., Antoshin, G. V., and Minachev, K. M., *J. Catal.* **107**, 522 (1987).
2. Kazuta, M., and Tanaka, K. I., *J. Catal.* **123**, 164 (1990).
3. Rodriguez-Ramos, I., Guerrero-Ruiz, A., Homs, N., Ramirez, de la Piscina, P., and Fierro, J. L. G., *J. Mol. Catal. A: Chemical* **95**, 147 (1995).
4. Haber, J., Janas, J., Schiavello, M., and Tilley, R. J. D., *J. Catal.* **82**, 395 (1983).
5. Yamaguchi, T., Tanaka, Y., and Tanabe, K., *J. Catal.* **65**, 442 (1980).
6. Baker, B. G., and Clark, N. J., *Stud. Surf. Sci. Catal.* **30**, 483 (1987).
7. Gielgens, L. H., Van Kampen, M. G. H., Broek, M. M., Van Hardeveld, R., and Ponec, V., *J. Catal.* **154**, 201 (1995).
8. Xing Cheng, Z., and Ponec, V., *Catal. Lett.* **25**, 337 (1994).
9. Thomas, R., Van Oers, E. M., De Beer, V. H. J., Medema, J., and Moulijn, J., *J. Catal.* **76**, 241 (1982).
10. Gilillambias, F. J., Salvatierra, J., Bouyssieres, L., Escudey, M., and Cid, R., *Appl. Catal.* **59**, 185 (1990).
11. Bosch, H., and Janssen, F., *Catal. Today* **2**, 369 (1988).
12. Ogata, E., Kamiya, Y., and Ohta, N., *J. Catal.* **29**, 296 (1973).
13. Katrib, A., Hemming, F., Wehrer, P., Hilaire, L., and Maire, G., *J. Elect. Spectrosc. Relat. Phenom.* **76**, 195 (1995).
14. Katrib, A., Logie, V., Saurel, N., Wehrer, P., Hilaire, L., and Maire, G., *Surf. Sci.* **377**, 754 (1997).
15. Katrib, A., Logie, V., Peter, M., Wehrer, P., Hilaire, L., and Maire, G., *J. Chim. Phys.* **94**, 1923 (1997).
16. David Jackson, S., Brandreht, B. J., and Winstanley, D., *App. Catal.* **27**, 325 (1986).
17. Zhang, R., Schwarz, J. A., Datye, A., and Baltrus, J. P., *J. Catal.* **138**, 55 (1992).
18. L'Argentière, P. C., and Figoli, N. S., *Catal. Lett.* **53**, 149 (1998).
19. Juan, A., Moro, C. C., and Damiani, D., *Colloid Surf. A* **122**, 257 (1997).
20. Plummer, H. K., Shinozaki, Jr. S., Adams, K. H., and Gandhi, H. S., *J. Mol. Catal.* **20**, 251 (1983).
21. Adams, K. M., and Gandhi, H. S., *Ind. Eng. Chem. Prod. Res. Dev.* **22**, 207 (1983).
22. Hoang-Van, C., and Zegaoui, C., *App. Catal. A General* **130**, 89 (1995).
23. Larsen, G., Lotero, E., Raghavan, S., Parra, R. D., and Querini, C. A., *App. Catal. A General* **139**, 201 (1996).
24. Hino, M., and Harata, K., *App. Catal. A General* **168**, 151 (1998).
25. Benson, J. E., Kohn, H. W., and Boudart, M., *J. Catal.* **5**, 307 (1966).
26. Bond, G. C., and Tripathi, J. B. P., *J. Less Common Metals* **36**, 31 (1974).
27. Bond, G. C., and Tripathi, J. B. P., *J. Chem. Soc. Faraday Trans. I* **72**, 933 (1970).
28. Khobiar, S., *J. Phys. Chem.* **68**, No. 2, 411 (1964).
29. Vaudagna, S. R., Comelli, R. A., and Figoli, N. S., *App. Catal. A General* **164**, 265 (1997).
30. Michalowicz, A., "Méthodes et Programmes d'Analyses des Spectres d'Absorption des Rayons X," Thesis. Paris, 1990.
31. Doniach, S., and Sunjic, M., *J. Chem. C* **3**, 285 (1978).
32. Regalbuto, J. R., Fleish, T. H., and Wolf, E. E., *J. Catal.* **107**, 114 (1987).
33. Biloen, P., and. Pott, G. T., *J. Catal.* **30**, 169 (1973).
34. Fiedor, J. N., Proctor, A., Houalla, M., and Hercules, D. M., *Surf. Int. Anal.* **23**, 204 (1995).
35. Haber, J., Stoch, J., and Ungier, L., *J. Solid State Chem.* **19**, 113 (1976).
36. Colton, R. C., and Rabalais, J. W., *Inorg. Chem.* **15**, No. 1, 236 (1976).
37. Hollinger, G., and Duc, T. M., *Phys. Rev. Lett.* **37**, No. 23, 1564 (1976).
38. Fleisch, T. H., and Mains, G. J., *J. Chem. Phys.* **76**, No. 2, 780 (1982).
39. Wachs, I. E., Chersich, C. C., and Hardenbergh, J. H., *App. Catal.* **13**, 335 (1985).
40. Ng, K. T., and Hercules, D. M., *J. Phys. Chem.* **80**, No. 19, 2094 (1976).
41. Salvati, L., Jr., Makovsky, L. E., Stencel, J. M., Brown, F. R., and Hercules, D. M., *J. Phys. Chem.* **85**, 3700 (1981).
42. Kerkhof, F. P. J. M., Moulijn, J. A., and Heeres, A., *J. Electr. Spectrosc. Relat. Phenom.* **14**, 453 (1978).
43. De Angelis, B. A., and Schiavello, M., *J. Solid State Chem.* **21**, 67 (1977).
44. Salje, E., Carley, A. F., and Roberts, M. W., *J. Solid State Chem.* **29**, 237 (1979).
45. Gehlig, R., Salje, E., Carley, A. F., and Roberts, M. W., *J. Solid State Chem.* **49**, 318 (1983).
46. Chappell, P. J. C., Kibel, M. H., and Baker, B. G., *J. Catal.* **110**, 139 (1988).
47. Cheval, M., Thesis. Strasbourg, 1992.
48. Muller, A., Thesis. Strasbourg, 1997.
49. Vannice, M. A., Boudart, M., and Fripiat, M. M., *J. Catal.* **17**, 359 (1970).
50. Vermaire, D. C., and Van Berge, P. C., *J. Catal.* **116**, 309 (1989).
51. Scheffer, B., Molhoek, P., and Moulijn, J. A., *App. Catal.* **46**, 11 (1989).
52. Kadkhodayan, A., and Brenner, A., *J. Catal.* **117**, 311 (1989).
53. Thomas, R., De Beer, V. H. J, and Moulijn, J. A., *Bull. Soc. Chim. Belg.* **90**, No. 12, 1349 (1981).
54. Thomas, R., Van Oers, E. M., De Beer, V. H. J., Medema, J., and Moulijn, J. A., *J. Catal.* **76**, 241 (1982).
55. Sancier, K. M., *J. Catal.* **23**, 301 (1971).
56. Fouad, N. E., Attyia, K. M. E., and Zaki, M. I., *Powder Tech.* **74**, 31 (1993).
57. Sahle, W., and Berglung, S., *J. Less-Common Metals* **79**, 271 (1981).
58. Arnoldy, P., De Jong, J. C. M., and Moulijn, J. A., *J. Phys. Chem.* **89**, 4517 (1985).
59. Schubert, W. D., *J. Ref. Hard Metals* **9**, No. 4, 178 (1990).
60. Zou, Z., *J. Ref. Hard Metals* **7**, No. 1, 57 (1990).
61. Kuzmin, A., and Purans, J., *J. Phys. IV* **7**, 999 (1997).
62. Vihnol, A. D., Sapre, V. B., and Mande, C., *J. Phys. Chem.* **52**, No. 8, 92163 (1991).
63. Dicko, A., Song, X., Adnot, A., and Sayari, A., *J Catal.* **150**, 254 (1994).
64. Tanuma, S. T., Powell, C. J., and Penn, D. R., *Surf. Int. Anal.* **17**, 911 (1991).